

# Further Experimental Evidence of the *Dead Matter Has Memory* Conjecture in Capacitive Devices

Anis Allagui<sup>1,2</sup>, Di Zhang<sup>1</sup> and Ahmed Elwakil<sup>3,4</sup>, *Senior Member IEEE*

<sup>1</sup>Dept. of Sustainable and Renewable Energy Engineering, University of Sharjah, United Arab Emirates (aallagui@sharjah.ac.ae)

<sup>2</sup>Dept. of Mechanical and Materials Engineering, Florida International University, Miami, FL33174, USA

<sup>3</sup>Dept. of Electrical Engineering and Computer Science, Khalifa University, United Arab Emirates (elwakil@ieee.org)

<sup>4</sup>Dept. of Electrical and Software Engineering, University of Calgary, Alberta, Canada (ahmed.elwakil@ucalgary.ca)

**Abstract**—This study provides new sets of experimental results supporting Westerlund’s conjecture that *Dead Matter Has Memory* [1]. Memory effects in the dynamic response of electric double-layer capacitors (EDLCs) that integrate its prior history of stimulation and state have been experimentally observed and reported in a few recent studies. The different excitation signals used to quantify such effects in these studies aimed at charging a device to the same voltage value and the exact same accumulated charge level but in different manners. Having reached the same unique voltage-charge point, it was observed that different yet repeatable discharge patterns occur, proving the existence of memory. The aim of this work is to provide further experimental evidence of the inherent memory effect in EDLCs in response to time-varying stationary input excitations with different statistical properties. In particular, different sets of charging voltage waveforms composed of fixed dc values with superimposed uniformly-distributed random fluctuations of different amplitudes were created and used to charge the same EDLC device to a unique voltage-charge point. The duration of these signals was the same but with different values of variance around the mean value. We observed different time-charge responses depending on the extent of the noise level in these charging waveforms. This is interpreted and discussed in the context of inherent memory using fractional-order voltage-charge equations of non-ideal capacitors.

**Index Terms**—Double-layer capacitors; Memory effect; Fractional-order capacitors

## I. INTRODUCTION

Over 30 years ago, Westerlund [1] highlighted the memory effect in non-ideal capacitors that follow power-law (dis)charge dynamics giving rise to the conclusion that dead matter must have memory. In a follow-up article, Westerlund and Ekstam [2] established the mathematical foundation of capacitor theory in the context of fractional-order calculus which cannot be avoided for the accurate modeling of non-ideal capacitive devices. The booming interest in fractional calculus and fractional-order dynamics has enabled more recent in-depth studies on the memory effect in dielectrics [3], neuron models [4], [5] and supercapacitors [6]. The experimental work done using supercapacitors in particular has provided solid proof of the existence of memory leaving no doubt to the validity of the *dead matter has memory conjecture* [7]. Supercapacitors are electrochemical energy storage devices known for their outstanding power performance, excellent reversibility and long cycle life, but they are still lagging

behind in terms of energy density when compared with batteries. Their charge storage mechanisms can be either physical, i.e. purely electrostatic ion adsorption in the electric double-layer at the electrode/electrolyte interface, or pseudocapacitive via highly reversible and relatively fast redox reactions, or both. Furthermore, the transport dynamics in such devices in response to an external excitation is mainly subdiffusive [8], which can be attributed to several factors including the porous nature of the electrodes, their fractal geometries and also because of internal friction forces and continuous scattering of ions diffusing in the supporting electrolytes and through the wetted pores [9]. In addition, different types of inter-ion interactions, crowdedness and buffering in narrow pores play a role in establishing retarded diffusion processes in these devices [8]. From a system-level perspective, the dynamics of supercapacitors follow a power-law behavior which can be viewed as the collective result of many coupled processes with different widely distributed time constants [10]. Multiple time scale dynamics hint at the existence of memory effects that take into account the global, non-local time behavior of past activities up to the present time. This type of behavior can be well described with fractional-order integro-differential equations [11], [12].

In recent years, there has been an intense effort to experimentally verify and quantify the memory effect in EDLCs. For example, in [7] it was shown that discharging a supercapacitor into a constant resistor from the same *voltage and charge* point reached using two different charging waveforms (step voltage and linear voltage ramp) of two different durations leads to two different responses, mostly in the short term, transient regime. This indicated that contrary to ideal capacitors, knowledge of the initial condition is not sufficient to determine the present and future states. In a second study [13], a quantitative estimate of memory using the voltage memory trace interpretation of fractional-order dynamics [5] was provided. A follow-up paper by the same group illustrated the application of the memory effect by sequentially encoding information into the charging pattern of the device, and then uniquely retrieving the coded information from the discharge response [14].

In this work, we further investigate the memory effect of supercapacitors, albeit in response to time-varying stationary voltage excitations. The input voltage waveforms are derived from uniform distributions of different sample ranges, means and variances. It is observed that the extent of the noisy exci-

tation around the mean value (i.e. the prehistory and features of the charging sequence) determine the actual response of the device at any given time. The cross correlation function between charge and voltage shows a visible degree of correlation, and thus short term memory effects, that fade out as the time lag is increased. We also allude to the effect of noise variance on the weighted sum memory trace that takes into account all prior history of the device. It is worth mentioning that in a recent study [15] aimed at explaining the *cardiac memory* where the electrical activity in the heart depends on the prior history of one or more system state variables the following was mentioned: *... Memory is represented via capacitive memory, due to fractional-order that arises due to non-ideal behavior of membrane capacitance.* Therefore, we believe that studying the memory effect in capacitive devices is of significant importance.

## II. THEORY

Consider a linear capacitive device characterized in the frequency domain (steady-state condition) by a capacitive system function  $C(s)$  ( $s = j2\pi f$  with  $f$  being the frequency), such that the charge-voltage relationship is given by:

$$Q(s) = C(s)V(s) \quad (1)$$

The corresponding time-domain charge-voltage relationship would then be represented in terms of a hereditary (convolution) integrals as [16], [17]:

$$\begin{aligned} q(t) &= \int_0^t c(t-\tau)v(\tau)d\tau = (c \otimes v)(t) \\ &= \int_0^t v(t-\tau)c(\tau)d\tau = (v \otimes c)(t) \end{aligned} \quad (2)$$

where the lower limit of the integrals can also be taken to be  $-\infty$  to reflect infinite past. Here in Eqs. 1 and 2,  $f(t) \leftrightarrow F(s)$  represents the pair of time-domain function  $f(t)$  and its frequency-domain Laplace transform  $F(s)$ , assumed to exist, i.e.  $\mathcal{L}\{f(t)\}(s) = F(s) = \int_{-\infty}^{\infty} f(t)e^{-st}dt$  and  $\mathcal{L}^{-1}\{F(s)\}(t) = f(t) = (2\pi j)^{-1} \int_{a-j\infty}^{a+j\infty} F(s)e^{st}ds$ . Analysis and discussions on these formulas and others for describing non-ideal capacitive devices can be found for instance in some of our recent work [18]–[20]. The integral in Eq. 2 indicates that the accumulated charge in the device at an instant  $t$  depends on the values of the applied voltage taken at times in the interval  $\tau \in [0, t]$  weighted by the convolution kernel  $c(t-\tau)$  characteristic of the device under study.

For the particular case of an ideal capacitor we write  $c(t-\tau) = C_1$  where  $C_1$  is a constant, independent of time or frequency. Thus, Eq. 2 simplifies to be the well-known relation

$$\Delta q(t) = C_1 \Delta v(t) \quad (3)$$

where  $\Delta q(t)$  is evidently equal to  $q(t) - q(0)$ , where  $q(0)$  is an initial arbitrary charge stored on the device. The same is for the voltage difference  $\Delta v(t)$ . Ideal capacitors are therefore said to be memoryless devices.

However, if the convolution kernel  $c(t-\tau)$  is not a constant, then all events over the history of the device contribute to its current state of charge. The capacitance of electrochemical

capacitors including EDLCs, pseudocapacitors and hybridized versions of the two cannot be taken as a constant. This is due to their complex structures, inhomogeneities and porosities of their electrodes, leading to distributed response times. These devices have been shown to exhibit fractional-order behavior [3], [6], [12], [21] that requires for their frequency-domain modeling invoking a fractional-order impedance function, e.g.:

$$Z_{\text{CPE}} = \frac{V(s)}{I(s)} = \frac{1}{C_\alpha s^\alpha} \quad (4)$$

Note that  $s^\alpha = \omega^\alpha \angle \alpha\pi/2$ , with  $0 < \alpha \leq 1$  and  $C_\alpha$  is in units of  $F s^{\alpha-1}$  [22]. The fractional-order capacitor is also known as the constant phase element (CPE) and its impedance reduces to that of an ideal capacitor  $1/(C_1 s)$  when  $\alpha = 1$ . The use of a fractional-order model indicates *a priori* that memory effects should be expected in time-domain experiments. We note in this regards that the time-domain voltage-current relationship corresponding to Eq. 4 is given, by inverse Laplace transform, by the integro-differential equation:

$$i(t) = C_\alpha {}_0^C D_t^\alpha v(t) \quad (5)$$

instead of the traditional ODE,  $i(t) = C_1 dv(t)/dt$ , known for ideal capacitors. The operator  ${}_0^C D_t^\alpha$  represents here the right-sided Caputo time fractional derivative of order  $\alpha > 0$ ,

$${}_0^C D_t^\alpha f(t) = \frac{1}{\Gamma(m-\alpha)} \int_0^t (t-\tau)^{-\alpha-1+m} f^{(m)}(\tau) d\tau \quad (6)$$

where  $m-1 < \alpha \leq m$ ,  $m \in \mathbb{N}$ , and  $f^{(m)}(\tau)$  is the  $m^{\text{th}}$  derivative of  $f(\tau)$  (in our case  $m = 1$ ). Again, this type of integrals indicate that all prior history of the function should be accounted for in order to determine the actual behavior of the device at the present time  $t$ . This can also be viewed from the finite difference approximation of Eq. 6. For  $t_k = k\Delta t$ ,  $k = 0, 1, \dots, K$  and using a time step  $\Delta t = T/K$ , then for all  $0 \leq k \leq K-1$  we have:

$${}_0^C D_t^\alpha v(t_{k+1}) \approx \frac{1}{\Gamma(2-\alpha)} \sum_{j=0}^k b_j \frac{[v(t_{j+1}) - v(t_j)]}{(\Delta t)^\alpha} \quad (7)$$

where  $b_j = [(k+1-j)^{1-\alpha} - (k-j)^{1-\alpha}]$ , with a  $(2-\alpha)$ -order accuracy in time [23]. We can rewrite Eq. 7 as:

$$\begin{aligned} {}_0^C D_t^\alpha v(t_{k+1}) \approx & \frac{(\Delta t)^{-\alpha}}{\Gamma(2-\alpha)} \{v(t_{k+1}) - v(t_k) + \\ & \sum_{j=0}^{k-1} b_j [v(t_{j+1}) - v(t_j)]\} \end{aligned} \quad (8)$$

which is the the sum of the immediate past of the voltage (first two terms, weighted by the Gamma function and the fractional time,  $(\Delta t)^\alpha$ ) and a memory trace [5] (summation term) that contains voltage information about all previous activity of the device. The memory trace term increases when the fractional order  $\alpha$  in Eq. 8 decreases further away from one [4], [13]. It is understood that at the limiting case of  $\alpha = 1$  (corresponding to first order integer derivative), the behavior of the differentiable function is determined only locally in an infinitesimal neighborhood of the considered point. In this case, the memory trace part vanishes, and does not have any

effect on the dynamics of the device [4], which is simply a memoryless capacitor.

Referring back to the convolution integrals and their system function kernels, the expression of the current represented by Eq. 6 with  $m = 1$  (i.e.  $0 < \alpha \leq 1$ ) can be written as the Laplace convolution:

$$i(t) = \frac{C_\alpha t^{-\alpha}}{\Gamma(1-\alpha)} \otimes \frac{dv(t)}{dt} \quad (9)$$

where the capacitive kernel is the power law function

$$c(t) = \frac{C_\alpha t^{-\alpha}}{\Gamma(1-\alpha)} \quad (10)$$

that tends to zero as  $t \rightarrow \infty$ . The charge-voltage relationship for these non-ideal capacitive devices in response to a voltage signal  $v(t)$  is not simply  $\Delta q(t) = C_1 \Delta v(t)$  (Eq. 3), but rather:

$$q(t) = \frac{C_\alpha t^{-\alpha}}{\Gamma(1-\alpha)} \otimes v(t) \quad (11)$$

or in discrete form:

$$\Delta q(t) = \frac{C_\alpha}{\Gamma(1-\alpha)} \sum_{j=0}^k (t-t_j)^{-\alpha} v(t_j) \quad (12)$$

This relation clearly indicates the presence of a memory effect in these devices [5].

### III. EXPERIMENT

The device under test for this study is a commercially-available GHC NanoForce supercapacitor, rated 1 F, 2.7 V, and the electrical measurements were conducted on a Biologic VSP-300 electrochemical station equipped with an impedance spectroscopy module<sup>1</sup>.

Before we analyze time-domain data, we first characterized the device by impedance spectroscopy. The results in terms of Nyquist representation of real vs. imaginary parts of impedance, and impedance phase angle vs. frequency at 0, 0.9, 1.8 and 2.7 Vdc are shown in Fig. 1. The figure shows a clear deviation of the spectral impedance of the device from that of an ideal capacitor. This impedance can be fitted good enough with an  $R_s$ -CPE model [7], [12], [14], which again suggests memory effects in time-domain measurements.

Secondly, the supercapacitor was charged using excitation voltage signals of the type

$$v(t) = v(t_0)H(t) + [v(t_1) - v(t_0)]H(t-t_1) + \dots + [v(t_j) - v(t_{j-1})]H(t-t_j) \quad (13)$$

where  $H(t-t_k)$  is the Heaviside step function. We used 64 different settings for  $v(t)$  by full factorial of (i) four different voltage mean values ( $V_{dc} = \mu = 0.5, 1.0, 1.5$  and  $2.0$  V) with (ii) four different ranges of uniformly-distributed voltage fluctuations (i.e.  $\pm 20, \pm 50, \pm 200$  and  $\pm 500$  mV) superposed on the dc values, and (iii) four different durations ( $\Delta t = 1, 5, 20$  and  $60$  seconds). It is clear that a uniform noise means the

<sup>1</sup>This instrument has a voltage resolution of  $1\mu\text{V}$  on  $60\text{mV}$ , voltage accuracy  $< \pm 1$  mV, and maximum voltage scan rate of  $0.2$  V/ms. Its current range is  $10$  nA to  $1$  A with lowest accuracy and resolution of  $\pm 100$  pA and  $0.8$  pA, respectively, on a  $10$  nA scale.

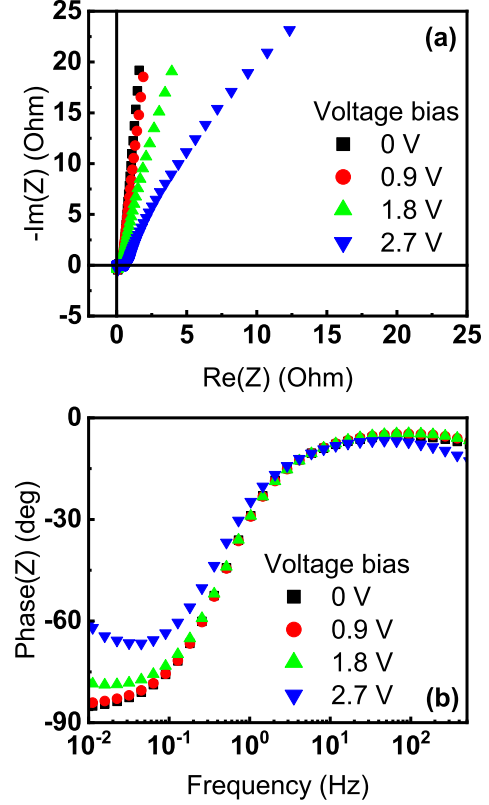


Fig. 1. Impedance spectroscopy results of the GHC NanoForce supercapacitor (rated 1 F, 2.7 V). Measurements were carried out on a Biologic VSP-300 electrochemical station using traditional stepped sine excitations of frequencies 10 mHz to 100 kHz with an amplitude of 10 mV around a given dc voltage, and the data were recorded at 10 frequency points per decade.

signal consists of values derived from a uniform distribution of probability density function expressed as

$$f(x) = \begin{cases} \frac{1}{b-a}, & a \leq x \leq b \\ 0, & \text{elsewhere} \end{cases} \quad (14)$$

with variance  $\sigma^2 = (b-a)^2/12$  taking the values of  $(0.13, 0.83, 13.3, \text{ and } 83.3) \times 10^{-3} \text{ V}^2$  for the ranges  $\pm 20, \pm 50, \pm 200$  and  $\pm 500$  mV, respectively. Each signal consisted of  $N = 1000$  points equispaced in time with a time step of  $\Delta t = T/N$ . Prior to each applied excitation, the supercapacitor was discharged down to 5 mV using a  $10 \Omega$  resistor.

### IV. RESULTS AND DISCUSSION

Typical results depicting the memory effect observed with the GHC NanoForce supercapacitor are shown in Fig. 2, corresponding to 20-seconds long, 0.5 V mean value voltage excitations with four different superposed uniformly-distributed fluctuations (see Fig. 2(a)). The last value of each charging sequence is appended to 0.5 V. The results obtained with the other dc voltage values and other time durations are similar to those in Fig. 2, and not shown here to preserve space. The accumulated charges in mA.h in response to the voltage excitations of Fig. 2(a) are shown in Fig. 2(b). The

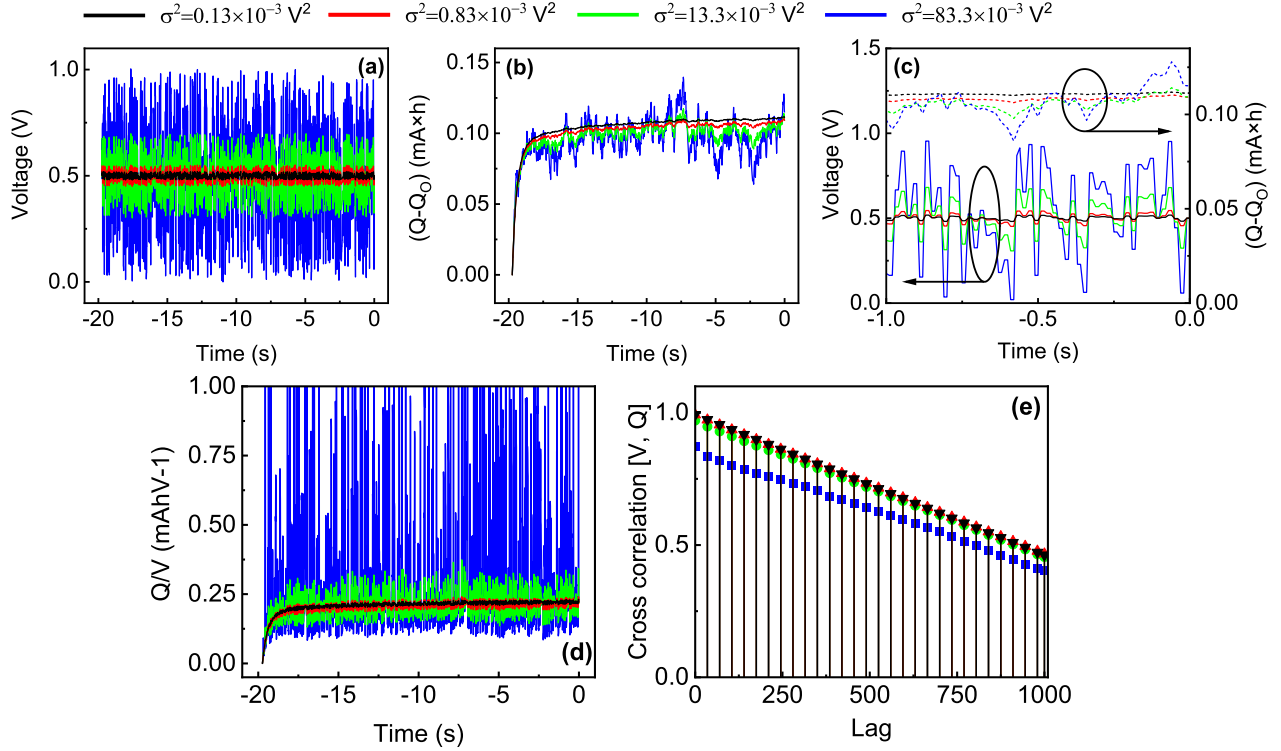


Fig. 2. (a) Applied time-domain voltage signals with a mean value of 0.5Vdc and (b) accumulated charge on the GHC NanoForce supercapacitor (rated 1F, 2.7V) when excited with these waveforms. (c) The synchronized voltage and charge vs. time for the last second of the experiment. (d) Plot of the ratio  $\Delta q/\Delta v$  vs. time and (e) plot of  $R_{vq}(\tau)$  (Eq. ??) vs. number of time lags

overall trends of the curves start first with a relatively quick power-law growth of the accumulated charge followed by an asymptotic limit as the charging time is increased [14]. We also observe from this quasi-stationary signal that in response to a sudden change of a voltage stimulus, the device responds accordingly with relatively large change in the instantaneous charge, followed by slower adaptation until the next change in voltage input (see Fig. 2(c)). The overall extent of change in the accumulated charge superposed on the general trend is accentuated by the increase in variance of the input voltage signal (Fig. 2(b) and Fig. 2(c)). This leads to the primary important conclusion that the device's accumulated charge adapts to changes in the stimulus statistics, not only in terms of its mean value but also in its variance.

Plots of the point-by-point ratios of charge to voltage are shown in Fig. 2(d). These results show also that by the end of the charging period, the overall accumulated charges are different from each other even though the last value of voltage was set to 0.5 V in all cases<sup>2</sup>.

In Fig. 2(e), plots of normalized cross-correlations between voltage and charge for the different levels of noise used are shown. The cross-correlation is defined as  $R_{vq}(\tau) = E\{v(t)q(t+\tau)\}$  where  $E\{\cdot\}$  denotes the expected value. The charge-voltage correlation as a function of time lag when the dc voltage input signal is superposed with the highly

fluctuating signal of  $\sigma^2 = 83.3 \times 10^{-3} \text{ V}^2$  always shows lower values compared to the cases with lower variance values. This indicates a lack of correlation between the two variables and thus the invalidity of the constitutive relation  $\Delta q(t) = C_1 \Delta v(t)$ , which applies for the case of ideal capacitors only [19]. Furthermore, the correlation coefficient defined as  $\rho_{vq} = \text{Cov}\{v, q\}/\sigma_v\sigma_q$  where  $\text{Cov}\{\cdot\}$  denotes the covariance between  $v$  and  $q$  are found to be -0.0491, -0.0297, 0.0684 and 0.2141 for the four different superposed signals respectively. The highest value of  $\rho_{vq}$  goes with the highest variance of noise. This is an indicator that the device remembers the extent of the noise level.

In connection with Eq. 12 which indicates that the memory trace term is more pronounced when the value of  $\alpha$  decreases, we note that the magnitude of non-dc frequency components of the voltage input  $v(t)$  increase with the increase of variance of the uniform noise (see DTFT of voltage excitations in Fig. 3). The stronger high-frequency components in the excitation signal are directly related to the increase of impedance phase angle in the device (i.e. lower value for  $\alpha$ ), as depicted in Fig. 1(b). Hence, the higher are the magnitudes of these frequency components, the stronger is the effect of the memory trace term in Eq. 12. To further verify this point, Eq. 12 was numerically executed with the same voltage signals applied experimentally on the supercapacitor device (Fig. 2(a)), and with  $C_\alpha$  and  $\alpha$  being 0.660 F sec $^{\alpha-1}$  and 0.905, respectively. These values are estimates of the CPE model parameters used

<sup>2</sup>The same is observed for the other tested scenarios, i.e. with different mean values and different excitation durations.

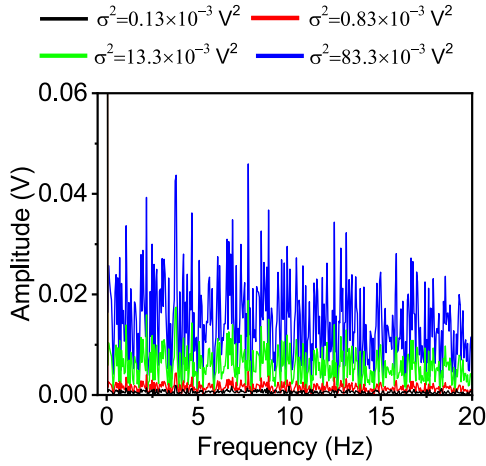


Fig. 3. Discrete-time Fourier transform (DTFT) of the applied charging voltage excitations depicted in Fig. 2(a)

to fit the impedance data measured at different dc voltage biases. The normalized cross-correlations between these voltage signals and their corresponding charges obtained via Eq. 12 are plotted in Fig. 4, and show similar trends to the experimental results (see Fig. 2(e)).

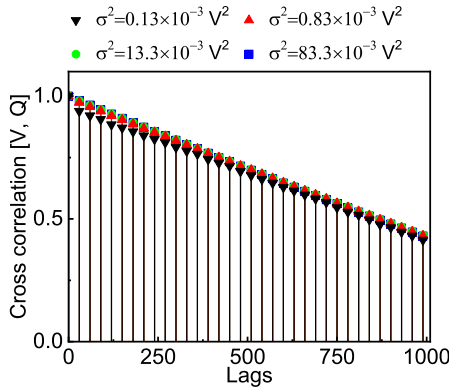


Fig. 4. Normalized cross-correlations between voltage and charge vs. number of time lags. The charge is obtained using Eq. 12 with  $C_\alpha = 0.660 \text{ F sec}^{\alpha-1}$ ,  $\alpha = 0.905$ , and with the same voltage signals applied experimentally on the supercapacitor device as depicted in Fig. 2(a)

lower values of the fractional coefficient  $\alpha$ , and thus with a

### V. CONCLUSION

In summary, we have provided further experimental evidence of the inherent memory effect in EDLCs which results from the complex multi-time scale dynamics of their internal microscopic structure and mechanisms. These results, in conjunction with those previously reported in [14], show that it is possible to encode information in the statistical distribution of the random noise signal superimposed on the dc step charging voltage of a device. From the fractional calculus modeling point of view, the memory effect in these devices is attributed to stronger higher frequency harmonics of the input signal, and as a consequence to the extent of deviation of the device from ideality. In other words, high variance fluctuations make the device operate in a less capacitive, more resistive mode with

stronger memory trace that integrates all past values of its state. We believe that there is no further doubt regarding the validity of the "dead matter has memory" conjecture [1].

### REFERENCES

- [1] S. Westerlund, "Dead matter has memory!" *Phys. Scr.*, vol. 43, no. 2, p. 174, 1991.
- [2] S. Westerlund and L. Ekstam, "Capacitor theory," *IEEE Transactions on Dielectrics and Electrical Insulation*, vol. 1, no. 5, pp. 826–839, 1994.
- [3] V. Uchaikin, R. Sibatov, and D. Uchaikin, "Memory regeneration phenomenon in dielectrics: the fractional derivative approach," *Physica Scripta*, vol. 2009, no. T136, p. 014002, 2009.
- [4] W. W. Teka, R. K. Upadhyay, and A. Mondal, "Fractional-order leaky integrate-and-fire model with long-term memory and power law dynamics," *Neural Netw.*, vol. 93, pp. 110–125, 2017.
- [5] W. Teka, T. M. Marinov, and F. Santamaria, "Neuronal spike timing adaptation described with a fractional leaky integrate-and-fire model," *PLoS Comput. Biol.*, vol. 10, no. 3, p. e1003526, 2014.
- [6] V. Uchaikin, A. Ambrozevich, R. Sibatov, S. Ambrozevich, and E. Morozova, "Memory and nonlinear transport effects in charging–discharging of a supercapacitor," *Technical Physics*, vol. 61, no. 2, pp. 250–259, 2016.
- [7] A. Allagui, D. Zhang, and A. S. Elwakil, "Short-term memory in electric double-layer capacitors," *Appl. Phys. Lett.*, vol. 113, pp. 253901–5, 2018.
- [8] R. Metzler and J. Klafter, "The random walk's guide to anomalous diffusion: a fractional dynamics approach," *Phys. Rep.*, vol. 339, no. 1, pp. 1–77, 2000.
- [9] H. Ribeiro and F. Potiguar, "Active matter in lateral parabolic confinement: From subdiffusion to superdiffusion," *Physica A*, vol. 462, pp. 1294–1300, 2016.
- [10] A. Allagui and H. Benaoum, "Power-law charge relaxation of inhomogeneous porous capacitive electrodes," *J. Electrochem. Soc.*, vol. 169, p. 040509, 2022.
- [11] M. Du, Z. Wang, and H. Hu, "Measuring memory with the order of fractional derivative," *Sci. Rep.*, vol. 3, p. 3431, 2013.
- [12] M. E. Fouda, A. Allagui, A. S. Elwakil, S. Das, C. Psychalinos, and A. G. Radwan, "Nonlinear charge-voltage relationship in constant phase element," *AEU - International Journal of Electronics and Communications*, vol. 117, p. 153104, 2020.
- [13] A. Allagui, D. Zhang, I. Khakpour, A. S. Elwakil, and C. Wang, "Quantification of memory in fractional-order capacitors," *J. Phys. D*, vol. 53, no. 02LT03, 2020.
- [14] A. Allagui and A. S. Elwakil, "Possibility of information encoding/decoding using the memory effect in fractional-order capacitive devices," *Sci. Rep.*, vol. 11, no. 1, pp. 1–7, 2021.
- [15] T. Comlekoglu and S. H. Weinberg, "Memory in a fractional-order cardiomyocyte model alters properties of alternans and spontaneous activity," *Chaos*, vol. 27, no. 9, p. 093904, 2017.
- [16] R. Nigmatullin, "On the theory of relaxation for systems with "remnant" memory," *Physica status solidi (b)*, vol. 124, no. 1, pp. 389–393, 1984.
- [17] D. Baleanu, A. K. Golmankhaneh, A. K. Golmankhaneh, and R. R. Nigmatullin, "Newtonian law with memory," *Nonlinear Dynamics*, vol. 60, no. 1, pp. 81–86, 2010.
- [18] A. Allagui, A. S. Elwakil, and C. Wang, "Time-domain and frequency-domain mappings of voltage-to-charge and charge-to-voltage in capacitive devices," *IEEE Trans. Circuits Syst. II Express Briefs*, vol. 70, no. 2, pp. 801–805, 2023.
- [19] A. Allagui, A. S. Elwakil, and M. E. Fouda, "Revisiting the time-domain and frequency-domain definitions of capacitance," *IEEE Trans. Electron Devices*, vol. 68, no. 6, 2021.
- [20] A. Allagui and M. E. Fouda, "Inverse problem of reconstructing the capacitance of electric double-layer capacitors," *Electrochim. Acta*, p. 138848, 2021.
- [21] A. S. Elwakil, A. Allagui, and C. Psychalinos, "On the equivalent impedance of two-impedance self-similar ladder networks," *IEEE Trans. Circuits Syst. II Express Briefs*, vol. 68, no. 7, pp. 2685–2689, 2021.
- [22] A. M. AbdelAty, A. S. Elwakil, A. G. Radwan, C. Psychalinos, and B. J. Maundy, "Approximation of the fractional-order laplacian  $s^\alpha$  as a weighted sum of first-order high-pass filters," *IEEE Trans. Circuits Syst. II Express Briefs*, vol. 65, no. 8, pp. 1114–1118, 2018.
- [23] Y. Lin and C. Xu, "Finite difference/spectral approximations for the time-fractional diffusion equation," *J. Comput. Phys.*, vol. 225, no. 2, pp. 1533–1552, 2007.